Наносистеми, наноматеріали, нанотехнології
Nanosystems, Nanomaterials, Nanotechnologies
2007, т. 5, № 1, сс. 105–116

PACS numbers: 78.20.Jq, 81.05.Je, 81.16.Hc, 81.16.Nd, 81.20.Ka, 82.45.Mp, 82.50.-m

Optical and Photoelectrochemical Properties of Nanostructured Materials Based on GaAs and WO_3

G. Ya. Kolbasov, S. V. Volkov, Yu. S. Krasnov, and I. A. Rusetskii

V. I. Vernadsky Institute of General and Inorganic Chemistry,
National Academy of Sciences of Ukraine,
32/34 Academician Palladin Blvd.,
UA-03142 Kyyiv, Ukraine

For semiconducting materials based on gallium arsenide and tungsten oxide as an example, the effect of nanostructurization of their surface and bulk on photoelectrochemical and electrochromic properties is shown.

На прикладі напівпровідникових матеріялів на основі арсеніду ґалію й оксиду вольфраму показано вплив наноструктурування їхньої поверхні та об'єму на фотоелектрохемічні і електрохромні властивості.

На примере полупроводниковых материалов на основе арсенида галлия и оксида вольфрама показано влияние наноструктурирования их поверхности и объёма на фотоэлектрохимические и электрохромные свойства.

Key words: gallium arsenide, photoelectrochemical processes, tungsten oxide, electrochromism, nanostructures.

(Received November 3, 2006)

1. INTRODUCTION

The physicochemical properties of semiconducting nanomaterials differ greatly from those of similar materials, which have no pronounced nanostructure or characteristic size. This related both to the set of their electrophysical, optical and luminescent properties and to the ability to exhibit a high electrocatalytic and photocatalytic activity in many chemical reactions [1–3]. This paper presents results of studying photoelectrochemical and electrochromic properties of materials based on gallium arsenide and tungsten trioxide with nanostructured surface or bulk. Salient features of these materials are a high quantum

yield of photoelectrochemical current (for GaAs electrodes [4, 5]) and pronounced electrochromic properties (for WO_3 films [6–8]), which makes them promising for use in electrochemical systems for solar energy conversion as well as in electrochromic and chemochromic displays and devices [5, 8–11].

2. EXPERIMENTAL

The nanostructurization of the GaAs surface with metals was performed by us by the electrochemical and photoelectrochemical methods [12–15]. For instance, to apply Pt nanoparticles to the GaAs surface with electronic conduction type, we employed the method of electrodeposition from a solution of chloroplatinic acid under strong semiconductor lighting in the fundamental light absorption region. Figure 1, *a* shows a micrograph of the surface of monocrystalline n-type GaAs modified by Pt nanoparticles. It was found that the diameter of platinum particles ranged between several nanometers to tens of nanometers, most particles having a mean diameter of $D \sim 10$ nm. Au and Zn nanoparticles were produced by cathodic electrodeposition at low current densities (10–20 $\mu A/cm^2$); to obtain Au, an $AuCl_3$ solution with addition of hydrofluoric acid was used, and Zn particles were deposited from an aqueous solution of $ZnCl_2$. The mean diameter of Au and Zn particles on the GaAs surface was $D = 6–10$ nm. CdS nanoparticles were deposited on GaAs during the formation of colloidal CdS particles in aqueous solution. To produce CdS nanoparticles, we used solutions containing cadmium citrate (or acetate) and sodium sulfide at a reagent concentration of 10^{-4}–10^{-2} mol/L; to stabilize the solution, gelatin was used; the deposition temperature was 20–22°C. To determine the size of colloidal CdS particles (D) in solution, a standard approach was used, which consists in de-

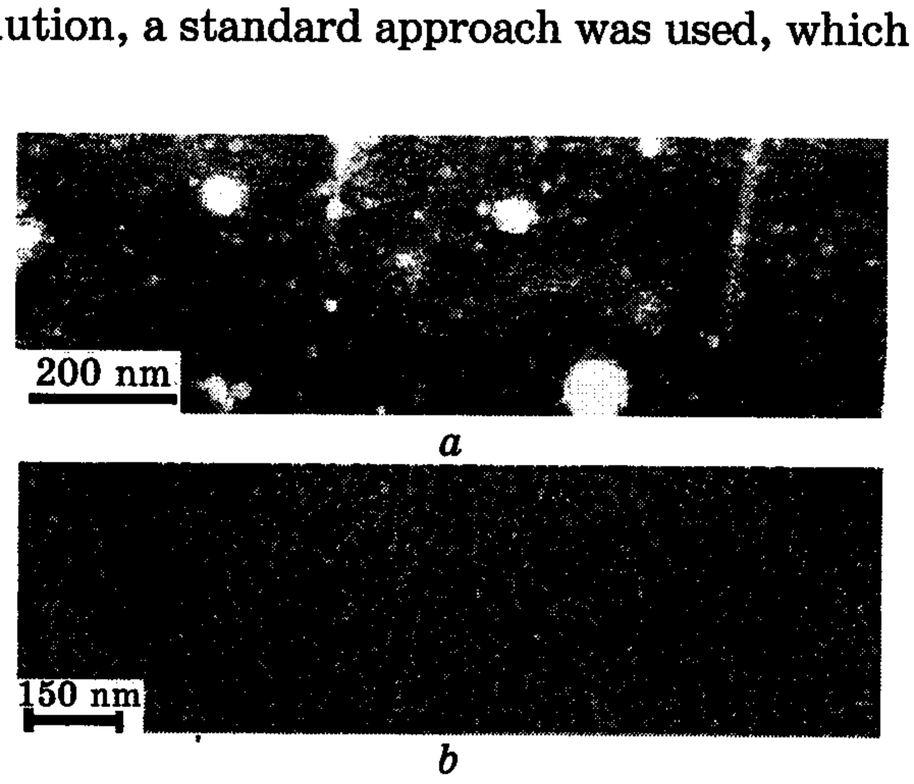

Fig. 1. Micrograph of the GaAs electrode surface (*a*, *b*) after nanostructurization with CdS (*a*) and Pt (*b*) particles.

termining the energy gap width of particles, E_g, from measurements of colloid absorption spectrum and calculation of the D value using the quantum-chemical calculations reported in reviews [1, 3, 9]. It was found that the mean particle diameter ranged between 1.3 and 5.5 nm, depending on the concentration of the starting reagents [16].

Figure 1, *b* shows micrographs of the GaAs surface after deposition of CdS nanoparticles; it is seen that these particles deposit on the surface uniformly as aggregates, whose mean size is larger by several fold than that of CdS particles in colloidal solution. The GaAs surface was studied by means of a 09-I-OC-10-005 Auger spectrometer and EM-200 electron microscope. The spectral dependences of photocurrent were measured in a quartz cell on a setup, which included an MDR-2 monochromator, and the light source was a DKSSh-500 xenon lamp with stabilized discharge current. The absorption spectra of CdS colloidal solutions were measured with a Specord UV–VIS spectrophotometer. The photoelectrochemical measurements have been made using a PI–50–1 potentiostat. The electrode impedance was measured with a Tesla BM 401 ac bridge. The solar energy conversion efficiency was determined in a polysulfide electrolyte of the composition 2 mol/l Na_2S + 2 mol/l NaOH + 1 mol/l S, in which GaAs is relatively stable. The electrode potential was measured with respect to a silver–chloride reference electrode.

a-WO_3 films were produced by cathodic electrodeposition from a Na_2WO_4-based aqueous electrolyte (0.2 M) with addition of 30% hydrogen peroxide (0.13 M) and H_2SO_4 (up to pH = 1). Deposition was performed in a transparent electrolytic cell with a platinum counter electrode at a constant cathode current density of 1 mA/cm^2 and a temperature of 23–25°C. *a*-WO_3 films were deposited on a transparent conducting SnO_2 film, spray deposited on a glass substrate, and on the polished surface of sheet tungsten. The design of the electrolytic cell allowed us to perform interferometric control of deposition : by recording interferograms simultaneously for two He–Ne laser beams with different angles of incidence on the electrode surface. Computer-aided analysis of these interferograms by the technique described in [17] enabled separate determination of current values of the thickness and refraction index of the growing *a*-WO_3 layer. By calculating from these interferograms the time dependence of the interfering beam that is specularly reflected by the surface of the growing film, one can determine the d dependence of the root-mean-square value of the size of its asperities and recesses [18].

The structure of as-prepared deposits was investigated by means of an x-ray diffractometer, an optical and scanning electron microscopes and by thermogravimetric method and infrared spectroscopy. The measurements of optical and electrochemical characteristics of the electrodes made were carried out in a transparent electrolytic cell, filled with 1*N* H_2SO_4, with a platinum counter electrode and silver-

cloride reference electrode, with respect to which all potential (E) values are given. The measurements were made on a PC-controlled units, which comprised an EP-21 potentiostat and an MDR-12 (LOMO) monochromator. The potential values and working-electrode current magnitudes were measured with V7-23 digital voltmeters with 0.2 s measurement time and an error of 0.01% of the upper measurement limit. The same voltmeter was used for periodical measurements of luminous flux level at the monochromator output (in the case of measuring transmission spectra, with an interval of 1nm), but because of noise and photomultiplier zero drift the error of such measurements at the photoresponce maximum was ~ 0.1%.

The electrosorption spectra of films deposited on tungsten were measured on a setup similar to those for measuring electroreflectance spectra of semiconductors [17]. The electrode potential was set with superposition of an alternating signal of 0.1 V amplitude at 20 Hz frequency on its constant component (E_S). The alternating component of current from a photomultiplier, which was proportional to the change in the intensity of monochromatic light reflected by a-WO_3 electrode, was recorded using phase detection. The value of the constant component of this current was maintained at the same level by means of an electronic circuit controlling the photomultiplier supply voltage. In this case, the change in the intensity of reflected monochromatic light because of reversible coloration of a-WO_3 electrode was 2–3 orders of magnitude larger than that caused by change in reflection coefficient at the WO_3/electrolyte and WO_3/W interfaces. Therefore, we regarded experimental plots of the alternating component of photomultiplier current against λ in this work as electrosorption spectra of a-WO_3.

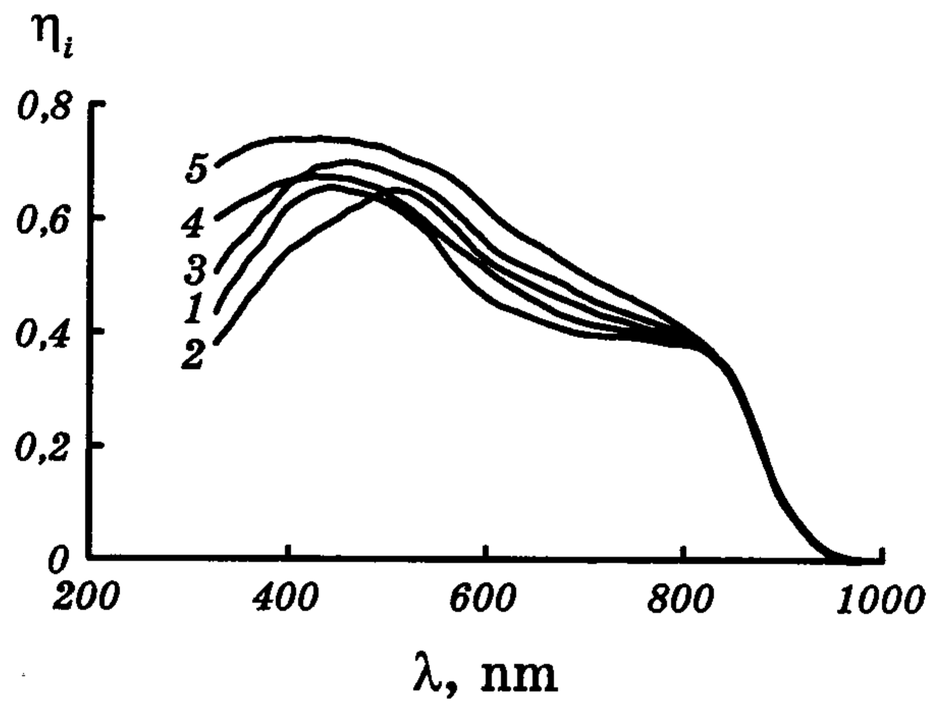

Fig. 2. Spectral dependence of the quantum yield of photoelectrochemical current, η_i, for a GaAs electrode, on whose surface Pt (*2*), Zn (*3*), Au (*4*) and CdS (*5*) nanoparticles have been deposited; (*1*) starting electrode. 1*N* KCl solution.

3. RESULT AND DISCUSSION

3.1. Photoelectrochemical Properties of Nanostructured GaAs Electrode

The nanostructurization of the gallium arsenide surface with metal and CdS particles affected greatly in some cases the photoelectrochemical properties of GaAs. Figure 2 shows the spectral dependence of the quantum yield of photoelectrochemical current, η_i , for GaAs electrode. A decrease in η_i in the short-wavelength region of the spectrum (Fig. 2, curve *1*) is characteristic of the starting GaAs electrode, on whose surface there were no nanoparticles [4, 19]. It was found that nanostructurization of the surface led to an increase in η_i in a wide spectral range. The largest increase in η_i was observed in the case of CdS (Fig. 2, curve *5*) and the smallest for Au (Fig. 2, curve *4*). After the deposition of Pt nanoparticles, an increase in η_i in the visible region and its decrease in the ultraviolet region were observed (Fig. 2, curve *2*).

The analysis of photoelectrochemical current (I_Φ) magnitude as a function of anodic photoelectrochemical reaction rate k_s^a, hole surface — recombination rate S_p and parameters of semiconductor (in this particular case *n*-type semiconductor) was performed according to the theory of photogenerated carrier transport across the semiconductor-electrolyte interface [5]:

$$I_\Phi = e\Phi\left\{\frac{1-e^{-Kl}/\left(1+KL_p\right)+\dfrac{kT}{eF_sL_p}\left(1-e^{-Kl}\right)}{1+\dfrac{kT}{eF_sL_p}+\dfrac{D_pe^{-Y_s}}{L_p\left(S_p+k_s^a\right)}}\right\}-i_c. \qquad (1)$$

Here Φ is the light intensity, F_s is the electric field at the semiconductor surface, D_p and L_p are the diffusion coefficient and diffusion length of minority carriers (holes) respectively, l is the width of space-charge region (SCR) near the semiconductor surface [5], K is the luminous semiconductor absorptivity, which depends on the optical wavelength λ, Y_s is the potential drop in the semiconductor SCR (in kT/e units), i_c is the photocurrent of cathodic photoelectrochemical reaction involving majority carriers. The expression for i_c is in this case [4, 5]:

$$i_c = \frac{e\Phi K}{K+eF_s/kT}\left[1+\frac{eF_sD_n}{kT(S_n+k_s^c)}\right]^{-1}. \qquad (2)$$

Here k_s^c is the rate of cathodic reaction, S_n is the rate of surface recombination of electrons, D_n is the diffusion length of electrons. The increase in the quantum yield of photocurrent, η_i, in the visible region after the nanostructurization of the Pt, Zn, CdS and Au surface (Fig.

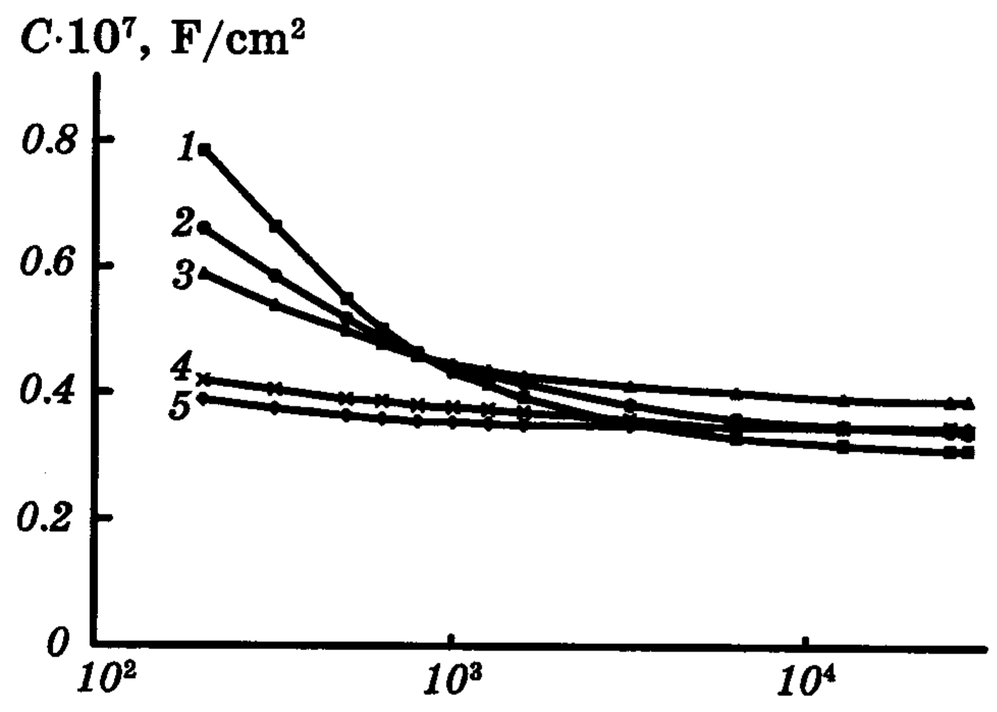

Fig. 3. Frequency dependence of differential capacity C of GaAs electrode nanostructured with Zn (*2*), Au (*3*), Pt (*4*) and CdS (*5*); (*1*) starting electrode. Solution: 2 mol/l Na_2S + 2 mol/l NaOH + 1 mol/l S. $E = -0.4$ V.

2) may be accounted for by an increase in the rate of surface recombination of holes, S_p, and hence by an increase in anodic photocurrent [4, 5, 16]. In the ultraviolet region, the luminous absorptivity K for GaAs increases [20], therefore the experimentally observed decrease in η_i in this region for starting GaAs is usually attributed to an increase in the contribution of cathodic photocurrent i_c [4, 5]. As follows from expression (2), the i_c value depends both on the cathodic reaction rate k_s^c and on the rate of surface recombination of electrons, surface electronic states being also involved in the electron transfer across the interface for the case where $S_p \neq S_n$ [4, 5].

Analysis of experimental data using expression (2) for the typical characteristics of GaAs [12, 13, 16] shows that after Pt surface modification, an additional increase in the rate of cathodic reaction (hydrogen evolution reaction in this particular case) must take place along with the decrease in surface recombination rate. After the deposition of Pt nanoparticles, the hydrogen evolution overpotential decreased substantially, which was caused by an increase in the catalytic activity of the nanostructured Pt surface. At the same time, the CdS, Au and Zn nanoparticles deposited on the GaAs surface had a lower catalytic activity in the hydrogen evolution reaction as against platinum and led to a decrease in surface recombination, as a result of which the total photocurrent in the short-wavelength region of the spectrum increased (Fig. 2, curves *3*–*5*). A decrease in surface recombination rate after the nanostructurization of GaAs electrode is also indicated by a decrease in the frequency dependence of differential capacity C, measured according to a parallel equivalent circuit (Fig. 3). From capacity measurements, one can determine the concentration of surface electronic states

(SES), N_t, on GaAs after its modification by Pt nanoparticles. The N_t quantity was defined as follows:

$$N_t = \frac{kT\Delta C}{e^2\theta(1-\theta)}, \tag{3}$$

where θ is the electron population of SES's ($\theta = 0.5$ when SES's are not involved in the electrochemical reaction [21]), $\Delta C = C_l - C_{SCR}$ is the difference between low-frequency capacitance (the calculations were made for $f = 200$ Hz (Fig. 3)) and SCR capacitance, determined at $f = 30$ kHz. It was found that the electronic state concentration determined in this way was lowest after the deposition of CdS and Pt nanoparticles on the GaAs surface and was $N_t = (0.3–0.5)\cdot 10^{10}$ cm^{-2}, whereas the SES concentration on starting samples was higher by an order of magnitude. This effect of nanoparticles on recombination processes may accounted for by the fact that they deposit mainly on active centres on the surface, which are formed by surface defects of different types or surface oxides, and are charge carrier recombination or trapping centres [21]; they neutralize the action of these centres by reducing their concentration and changing their energetics and electron and hole trapping coefficients. After the nanostructurization of the GaAs electrode surface the efficiency of the conversion of solar to electrical energy in polysulfide solution reached 23–24%.

3.2. Electrochromic Properties of Nanostructured *a*-WO_3

According to the results of investigations by XRD, TEM and TG-DTA, which were given earlier in [17], the deposited films are x-ray amorphous and strongly hydrated because they contain a large number of coordinately linked (up to 15 wt.%) and free water molecules. The specific density of such films is less than 50% of the density of crystalline WO_3, which agrees with the low value of their refraction index, $n = 1.6–1.7$ (at $n = 2.5$ for crystalline WO_3). The presence of an intense peak at 950 cm^{-1} in the IR absorption spectra of the deposit (as a specially prepared powder) indicates that these are many end atoms with double bond of the W=O type.

Since formation of polytungstate ions with 12 tungsten atoms (Keggin nanostructure), such as $H_2W_{12}O_{40}^{6-}$ [22], is characteristic of acidic Na_2WO_4 solutions, the presence of these ions may also be expected in the structure of deposited WO_3. On acidification, a precipitate of colloidal $WO_3\cdot 2H_2O$ particles is gradually formed in such a solution. The joining of these particles to larger associates during deposition on a substrate can be prevented by the addition of an oxalic acid solution. As is shown in Fig. 4, the size of the deposited colloidal particles decreases in this case to several nanometers.

Fig. 4. Micrograph of the appearance of a precipitate of colloidal tungsten oxide particles obtained from a Na_2WO_4 solution.

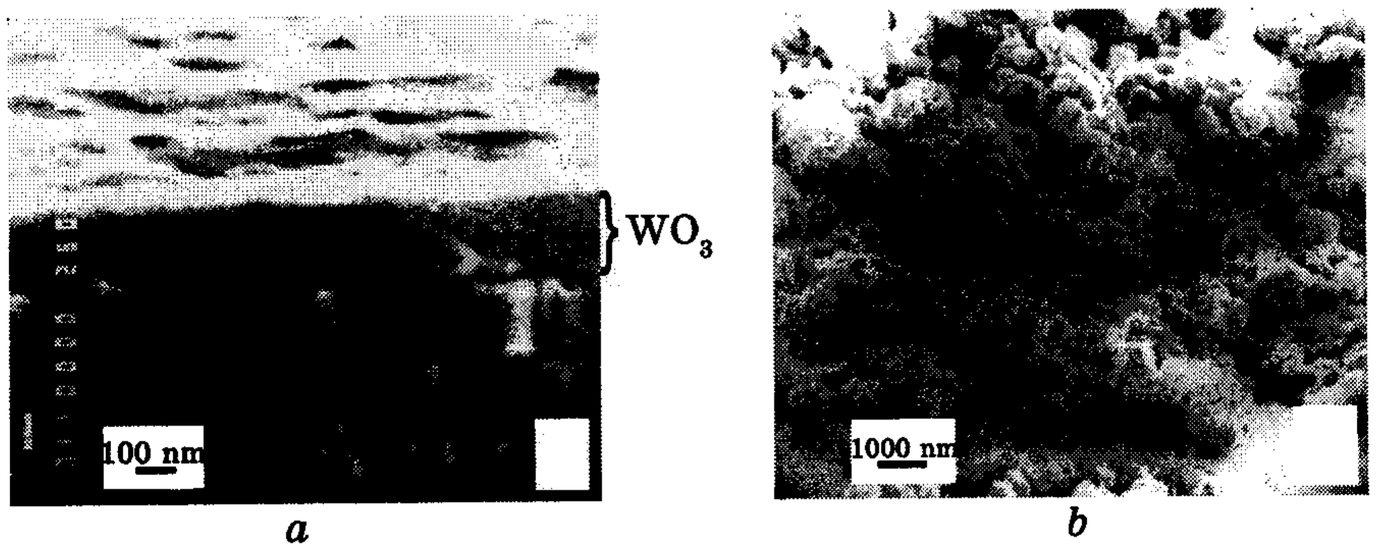

Fig. 5. SEM pictures of a cathodically deposited a-WO_3 films: (a) thin film deposited at a current density of 1 mA/cm^2 (view in the region of fracture on the substrate); (b) thick film deposited at 3 mA/cm^2.

The cycling of films after deposition in 1N H_2SO_4 showed that the rapidity of the coloration process at $\lambda = 625$nm up to $E = -0.4$ V was ~ 0.1 s at a contrast of ~ 80%. In this case, the value of charge injected into the film is $Q \approx 14$ mC/cm^2, and the coloration efficiency is ~ 50 cm^2/C. Figure 5, a shows a scanning electron micrograph of such a film in the fracture region on the substrate. At a small thickness, when $d \leq 0.5$ μm , the micrograph shows no cathode deposit structure. The film looks homogeneous, with a smooth surface, whose quality is comparable to that of the SnO_2 layer surface. At higher current density values (3–10 mA/cm^2), the cathode deposits had a very extended surface with a great number of defects as dendoide-like protrusions and a poor adhesion to the substrate and were characterized by a much lower coloration rapidity. The deposition of them was accompanied by a decrease in the intensity of light beam reflected by the film surface due to scattering by inhomogeneities, whose linear dimensions are comparable to λ (Fig. 5, b).

To establish the nature of the colour centres in cathodically deposited a-WO_3, studies of the dependence of absorption spectra of films on their potential in 1N H_2SO_4 were carried out together with measurement of current–potential curves for the coloration–decoloration proc-

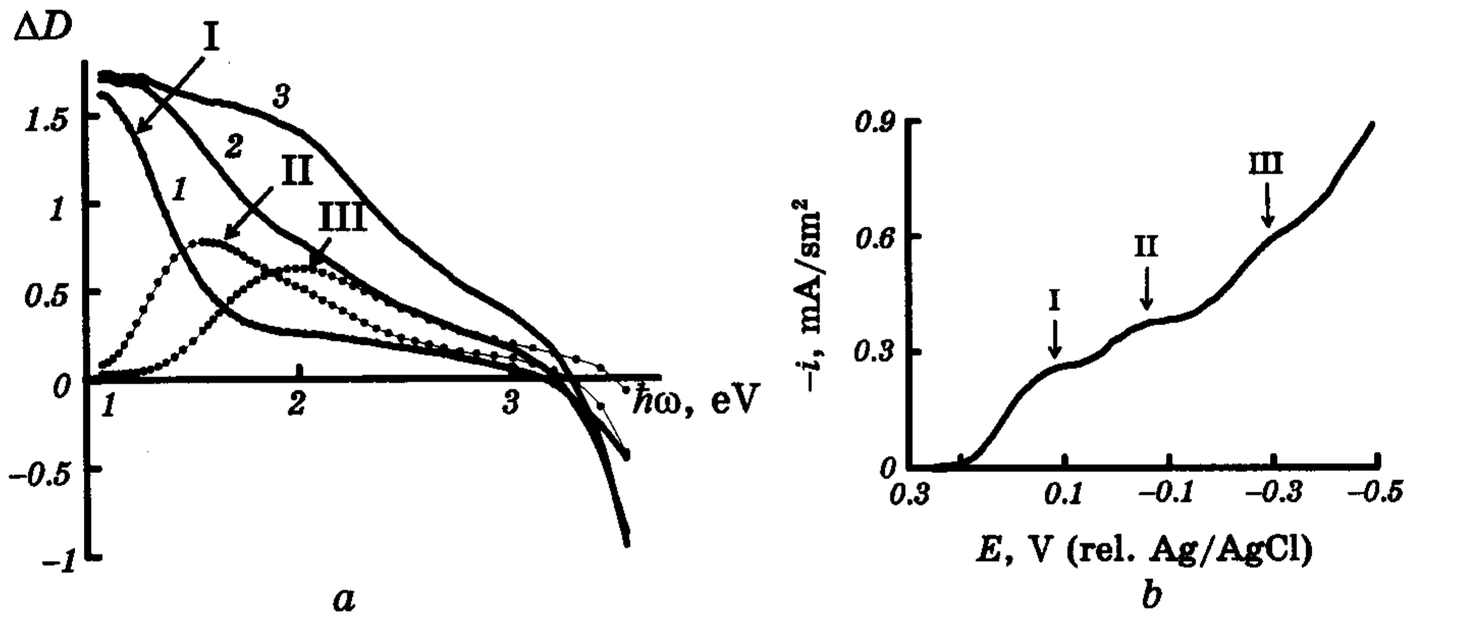

a *b*

Fig. 6. Coloration spectra of an *a*-WO_3 film 1 μm in thickness (*a*) at a potential of 0 V (*1*), –0.2 V (*2*), –0.4 V (*3*) (the points denote the coloration difference spectra of the film in potential ranges of 0.4 to 0 V (I), 0 to –0.2 V (II), –0.2 to –0.4 V (III)) and dependence of coloration current on potential in the course of its sweep in the cathodic direction at a rate of 10 mV/s (b).

ess at different potential sweep rates [23, 24]. Figure 6, *a* (curves *1*, *2*, *3*) shows the spectral distribution of optical density for absorption, $\Delta D(\hbar\omega)$, which appears in the course of coloration of an *a*-WO_3 film 1 μm in thickness at potential values between $E = 0.4$ V (for which $D = 0$) and $E = 0$ V, –0.2 V and –0.4 V respectively. In the initial stage of coloration, when the potential varies between $E = 0.4$ V and $E = 0$ V, an intense absorption band with a maximum at $\hbar\omega \approx 1$ eV appears in the optical spectrum of the film. But as E varies from 0 V to –0.4 V the D value trends towards saturation in the region of this band's maximum, and the absorption in the shorter-wavelength region of the spectrum continues to increase through the reduction of other W(VI+) centers with higher position of their unoccupied *d*-orbital on the energy scale.

The contribution of these W(VI+) centres to the absorption by the cathodically deposited film in the potential ranges 0 to –0.2 V and –0.2 to –0.4 V is shown by the difference absorption spectra II and III in Fig. 6, *a*, which were obtained by subtracting spectrum 1 from spectrum 2 and spectrum 2 from spectrum 3. These difference spectra exhibit sequential appearance of two more absorption bands with maxima at $\hbar\omega \approx 1.6$ eV and 2 eV, which is a characteristic sign of reduction of polytungstate ions with Keggin structure by one and then another electron [22]. In such ions of about 1 nm size, each of the 12 tungsten atoms has one W=O bond with end oxygen atom. In the volt–ampere curve for the coloration process (Fig. 6, *b*), three consecutive cathode current build-up portions correspond to the three above optical absorption bands. The bulk of the electrons injected into the film is spent on the reduction of polytungstate ions in it and on the formation of type II

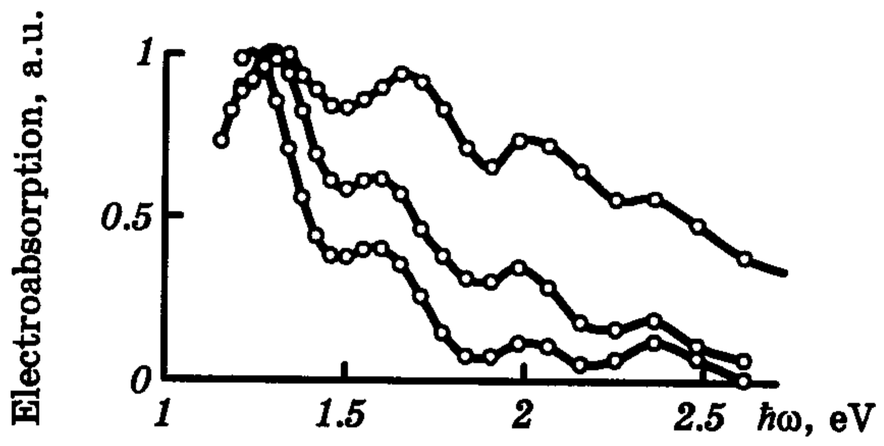

Fig. 7. Normalized electroabsorption spectra of a cathodically deposited a-WO_3 film 0.08 μm in thickness at potentials of 0.3 V (*1*), 0 V (*2*), –0.3 V (*3*).

and III colour centres (Fig. 6, *b*), indicating predominance of such complex anions in the structure of cathodically deposited a-WO_3.

The assignment of the optical absorption bands with maxima at 1.6 eV and 2 eV to reduced polytungstate ions is supported by the electroabsorption spectra of cathodically deposited a-WO_3 shown in Fig. 7. The absorption bands in these spectra are identical to those typical of most reduced polytungstate ions with Keggin nanostructure [22, 25]. Taking into account the data given in [26, 27], the appearance of a longer-wavelength intense absorption band with ~ 1 μm maximum in the initial stage of film coloration may be attributed to the reduction of W(VI+) centers being part of larger clusters, where polytungstates are joined to associates of several nanometers size. In the region $\hbar\omega > 3$ eV, the quantity ΔD in Fig. 6, *a* transfers to the region of negative values, which corresponds to the 'bleaching' effect of cathodically deposited oxide through a gradual shift of its fundamental absorption edge towards higher quantum energies by $\Delta\hbar\omega \approx 0.42$ eV [17]. This corroborates the presence of polytungstate anions in it since a similar shift of the absorption band that is associated with the same optical transitions is observed in the case of reduction of these anions in solution [25].

On the basis of nanostructured a-WO_3 films covered with a thin layer of platinum, we have made and investigated prototypes of optical hydrogen sensors [28]. The degree of coloration of such a sensor is determined by the percentage of H_2 in the air-hydrogen mixture. As the hydrogen concentration increases the light absorption by the a-WO_3 layer in the IR region with ~ 1 μm maximum trends towards saturation, whereas the absorption in the shorter-wavelength region of the spectrum continues to increase owing to the reduction of nanoclusters as polytungstate ions in cathodically deposited a-WO_3. Thanks to the strong light absorption by the film in the visible region, we managed to achieve a sensitivity of ~ 1% [H_2] for a sensor for the sight control of hydrogen content.

4. CONCLUSIONS

The results presented in this paper show that nanostructured materials

based on gallium arsenide and tungsten trioxide have properties that differ greatly from those of the materials having no nanostructured surface or bulk. Gallium arsenide based nanostructured photoelectrodes have a uniquely high photosensitivity and characteristics, which make it possible to use them in photoelectrochemical systems for solar energy conversion. We found that after the nanostructurization of the GaAs electrode surface, the efficiency of the conversion of solar to electrical energy in polysulfide solution reached 23–24%. Cathodically deposited *a*-WO_3 films, unlike films obtained by other methods, have a porous structure with polytungstate ions formed by 12 W atoms (Keggin nanostructure) predominating in it. The high degree of coloration in the visible region, which is typical of such films, contributes to higher efficiency of electrochromic devices and optical hydrogen sensors based on them.

REFERENCES

1. A. Hagfeld and M. Grätzel, *Chem. Rev.*, **95**, No. 1: 49 (1995).
2. M. R. Hoffmann, S. T. Martin, W. Choi et al., *Chem. Rev.*, **95**, No. 1: 69 (1995).
3. R. F. Khairutdinov, *Uspekhi Khimii*, **67**, No. 2: 125 (1998).
4. N. L. Dmitruk, G. Ya. Kolbasov, N. I. Taranenko et al., *Poverchnost. Fizika, Khimiya, Mekhanika*, No. 11: 34 (1985).
5. G. Ya. Kolbasov and A. V. Gorodyskii, *Photoinduced Charge-Transfer Processes in the Semiconductor–Electrolyte System* (Kiev: Naukova Dumka: 1993) (in Russian).
6. C. G. Granqvist, *Handbook of Inorganic Electrochromic Materials* (Amsterdam: Elsevier: 1995).
7. P. M. S. K. Monk, *Handbook of Advanced Electronic and Photonic Materials*, (San Diego: Academic Press: 2001), vol. **7**, p. 105.
8. M. A. Aegerter, *Sol–Gel Chromogenic Materials and Devices in Structure and Bonding* (Berlin: Springer Verlag: 1996), vol. **85**, p. 149.
9. A. L. Stroyuk, A. I. Kryukov, S. Ya. Kuchmii et al., *TEKh.*, **41**, No. 2: 67 (2005).
10. B. W. Faughnan and R. S. Crandall, α-WO-*Based Electrochromic Displays* (Ed. Zh. Pankov) (Moscow: Mir: 1982), p. 228.
11. B. W. Faughnan, R. S. Crandall, and P. M. Heyman, *RCA Rev.*, **36**, No. 1: 177 (1975).
12. I. A. Rusetskii, G. Ya. Kolbasov, D. B. Dan'ko et al., *Ukr. Khim. Zhurn.*, **70**, No. 9: 44 (2004).
13. G. Ya. Kolbasov, Yu. M. Solonin, I. A. Rusetskii et al., *Nanosystemy, Nanomaterialy, Nanotekhnologii*, **2**, No. 4: 1275 (2004).
14. Yu. M. Solonin, G. Ya. Kolbasov, I. A. Rusetskii et al., *NATO Science Series. II. Mathematics, Physics and Chemistry*, **202**: 193 (2005).
15. I. A. Rusetskii, G. Ya. Kolbasov, D. B. Dan'ko et al., *Ukr. Khim. Zhurn.*, **72**, No. 1: 62 (2006).
16. G. Ya. Kolbasov, S. V. Volkov, V. S. Vorobets et al., *Nanosystemy, Nanomaterialy, Nanotekhnologii*, **2**, No. 1: 169 (2004).
17. Yu. S. Krasnov and G. Ya. Kolbasov, *Electrochim. Acta.*, **49**: 2425 (2004).
18. Yu. S. Krasnov, A. T. Vasko, F. N. Patsyuk et al., *Ukr. Khim. Zhurn.*, **60**, No. 5–6: 418 (1994).

19. Ye. V. Kuzminskii and G. Ya. Kolbasov, *Solar Energy Materials & Solar Cells*, **56**: 93 (1999).
20. *Optical Properties of Semiconductors (A3B5-Type Semiconducting Compounds)* (Eds. R. Willardson and A. Bir) (Moscow: Mir: 1970).
21. Yu. V. Pleskov and Yu. Ya. Gurevich, *Semiconductor Photoelectrochemistry* (New York: Plenum Press: 1986).
22. M. S. Pop, *Heteropoly- and Isopolyoxometalates* (Novosibirsk: Nauka: 1990) (in Russian).
23. Yu. S. Krasnov, G. Ya. Kolbasov, V. N. Zaichenko et al., *Ukr. Khim. Zhurn.*, **71**, No. 11–12: 92 (2005).
24. S. V. Volkov, G. Ya. Kolbasov, Yu. S. Krasnov, *Visnyk Kharkivskogo Natsionalnogo Universytetu*, **12(35)**, No. 648: 134 (2005).
25. G. M. Varga, E. Papaconstantinou, and M. T. Pope, *Inorg. Chem.*, **9**, No. 3: 662 (1970).
26. G. A. Niklasson, J. Klasson, and E. Olsson, *Electrochim. Acta*, **46**: 1967 (2001).
27. S. Hashimoto and H. Matsuoka, *J. Appl. Phys.*, **69**: 933 (1991).
28. S. V. Volkov, G. Ya. Kolbasov, and Yu. S. Krasnov, *Research in the Field of Sensor Systems and Technologies. Conference-Report on the Comprehensive Basic Research Program of the Ukrainian National Academy of Sciences* (Kyyiv: 2005), p. 22 (in Ukrainian).